Sun Tracking PV Power Plants: Experimental Validation of Irradiance and Power Output Prediction Models

André Coelho* , Rui Castro*

*Centre for Innovation in Electrical and Energy Engineering (Cie3), IST – Technical University of Lisbon, Portugal,

‡ Corresponding Author; Av. Rovisco Pais,1049-001 Lisboa, Portugal, : +351 21 8417287, rcastro@ist.utl.pt, andre.coelho@ist.utl.pt

Received: 22.09.2011 Accepted:20.10.2011

Abstract- Unlike traditional power plants, where the power output is easily controlled, those based on uncontrollable intermittent renewable resources have an inherent uncertainty on its availability. In the case of photovoltaics, their output is not only dependent on the solar resource itself, but also on the cell's temperature and on the collection system. The purpose of this paper is to present a model that allows estimating the power produced by PV systems with solar tracking based on irradiance and temperature data related to fixed systems. To that end, the main concepts related to solar geometry and incidence angle computation are recalled and a PV power model (the one diode and five parameters model) is presented. The developed model is validated with experimental data collected in a PV test facility and with PVGIS records.

Keywords- Photovoltaics, solar collection, solar tracking, power output model.

1. Introduction

Issues like the depletion of ozone layer, global warming, oil prices, security of supply and the exhaustion of fossil reserves have triggered the need to increase the share of renewables in electrical energy generation. Solar energy is the most abundant energy resource on Earth. Over the past two decades, photovoltaic (PV) power has become well established in remote areas, where this technology is often the most cost-effective choice. On the other hand, PV systems are also becoming very common in grid-connected applications, as the technology improves and is achieving maturity. As a consequence of the performance of PV system components and the leverage of large-scale industrial production, a steady cost reduction is being observed.

Unlike traditional power plants, where the power output is easily controlled, those based on uncontrollable intermittent renewable resources have an inherent uncertainty on its availability. This makes investment decisions and system sizing difficult tasks. To circumvent this problem, theoretical models are commonly used to estimate the power produced by renewable systems based on its specifications and history of their renewable resources.

In the case of photovoltaics, their output is not only dependent on the solar resource itself, but also on the cell's temperature. Another issue to take into account is the absence of datasheet information allowing a direct relation between available power, solar resource and cell temperature. To overcome this problem, models which describe the electrical behaviour of the devices constituting the photovoltaic systems in terms of certain key factors must be developed.

Several models have been published in the literature addressing this issue. The simplest ones are based on an equivalent electrical circuit composed by a source current in parallel with a diode. These models are usually known as "one diode and three parameters" models (see, for instance, [1], [2]). More sophisticated models add some complexity to these simpler ones. One can then find one diode and four or five parameters models, depending on the level of resistive effects added ([3], [4], [5] are just some examples of developments on the five parameters model, mainly in what concerns the computation of the parameters). Furthermore, models with two parallel diodes can also be found in the literature (the main reference is [6]).

For the study reported in this paper, a "one diode and five parameters" PV power output prediction model was

selected, in which we have introduced some innovation on the technique used to evaluate the parameters. An important characteristic of this model is that it is derived based solely on datasheet information. Some work on this subject has been reported in [7], [8]. Another relevant feature of the model is that it is able to describe the behaviour of a PV system for any given irradiance and temperature conditions.

Another key aspect to consider in estimating the power produced by such systems is related with the solar collection mechanisms used. Thus, to correctly estimate the energy produced by these systems is necessary to know (or estimate) the irradiance and cell temperature for each solar collection topology. However, it is known that the existing records are normally obtained with fixed devices, limiting the study of other options, particularly those with tracking systems. Therefore, a technique to derive the relationship between readily available data obtained through measurement fixed systems and the maximum global irradiance that actually input the PV systems equipped with Sun tracking mechanisms is presented in this paper.

In short, the purpose of this study is to present a PV output prediction model that allows estimating the power produced by PV systems with solar tracking, based on data obtained by irradiance and temperature measurement fixed systems. Furthermore, this theoretical model is validated against experimental results obtained in a PV test apparatus composed by two generating units, one with a fixed system and the other with a two axes tracking system. Records of PVGIS (Photovoltaic Geographical Information System) database are also used to strengthen the validity of the presented model

2. Global Irradiance Prediction Model

In this section the maximum global irradiance prediction model based on data obtained by irradiance and temperature measurement fixed systems is presented. This calculation is important because the irradiation value that input ideal PV systems equipped with Sun tracking systems is the maximum global irradiance. For this purpose, some relevant aspects of the celestial dynamics are reviewed and the computation of the incidence angle is presented. This allows the maximum global irradiance (direct + diffuse) to be obtained from the total irradiance as measured by a fixed system.

2.1. Celestial dynamics

In order to understand how to collect energy from the Sun, it is imperative to predict the relation between the Sun's and the collection device's locations. Therefore, it is necessary to know the solar dynamics and the key indicators that define the relative positions of the Sun and the Earth. In this section, concepts that relate the passage of time with the movements of the Sun and the main angles used to determine the position of the Sun are recalled, according to [9].

Solar time

Solar time (t_s) is based on the 24 hour clock, with 12h00 as solar noon (the time that the Sun is exactly due south - in northern hemisphere, or due north - in the southern hemisphere). The concept of solar time is used in predicting the direction of sunrays relative to a point on the Earth. Solar time is location (longitude) dependent and is generally different from local clock time (LCT), which is defined by politically defined time zones and other approximations.

The conversion between solar time and local clock time requires knowledge of the location, the day of the year, and the local standards to which local clocks are set. It takes the form:

$$LCT = t_s - \frac{EOT}{60} + LC + D \tag{1}$$

In equation (1), LCT is in hours, EOT is the equation of time in minutes, LC is the longitude correction in hours and D is the daylight saving time parameter. All of these are defined in the following paragraphs.

1) Equation of time (EOT): Is the difference between mean solar time and true solar time on a given date. An approximation for calculating the equation of time is given by:

$$EOT = 0,258\cos x - 7,416\sin x - \\ -3,648\cos 2x - 9,228\sin 2x \tag{2}$$

Referring to equation (2), EOT is in minutes, N is the day number since January 1st and x (in degrees) is defined as a function of the day number N as . Details about the coefficients of equation (2) can be found in [10].

2) Longitude correction (LC): Is the parameter that reflects the difference between the time of the reference meridian and the time of the system's exact location. It is defined as (LC is in hours, g is the local longitude angle and LSTZ is the longitude of standard time zone meridian, both in degrees):

$$LC = \frac{\gamma - LSTZ}{15} \tag{3}$$

3) Daylight saving time parameter (D): Is a parameter that is equal to 1 (hour) if the location is in a region where daylight saving time is currently in effect, or zero otherwise.

Earth-Sun angles

In the following paragraphs it is defined a set of angles that allows to relate the position of both Earth and Sun: the hour angle and the declination angle.

1) The hour angle (w): To describe the Earth's rotation about its polar axis, the concept of hour angle is used. The hour angle is the angular distance between the meridian of the observer and the meridian whose plane contains the Sun. The hour angle is zero at solar noon and increases by 15º every hour. It is possible to define the hour angle as a function of solar time using the following expression:

$$\omega = 15\left(t_s - 12\right) \tag{4}$$

where t_s is the solar time in hours and w is in degrees.

2) The declination angle (d): The motion of the Earth around the Sun is pictured by the apparent motion of the Sun in the ecliptic which is tilted at 23,45º to the celestial equator. The angle between the line joining the centres of the Sun and the Earth and the equatorial plane is called the solar declination and denoted by δ. For most solar system design purposes the declination angle can be obtained by:

$$\delta = \sin^{-1}\left\{0,39795\cos\left[0,98563\left(N-173\right)\right]\right\} \quad (5)$$

where the argument of the cosine is in degrees and δ is in degrees.

Observer-Sun angles

When the Sun is observed from an arbitrary position on Earth, it is important to define the Sun's position relative to a coordinate system based at the point of observation, not at the centre of the Earth. The conventional Earth-surface based coordinates are a vertical line (straight up) and a horizontal plane containing a north-south line and an east-west line. The position of the Sun relative to these coordinates can be described by two angles: the solar altitude angle (a) and the solar azimuth angle (A).

The solar altitude angle is defined as the angle between the central ray from the Sun and a horizontal plane containing the observer. As an alternative, the Sun's altitude may be described in terms of the solar zenith angle (θz) which is the complement of the solar altitude angle.

The other angle defining the position of the Sun is the solar azimuth angle. It is the angle, measured clockwise on the horizontal plane, from the north-pointing coordinate axis to the projection of the Sun's central ray. Both the solar azimuth and the solar altitude angles will be dealt with in the next section.

2.2. Incidence angle

To take advantage of solar energy collection it is important to know the angle between the Sun and the surface of the photovoltaic collector, since the maximum amount of irradiance that can reach a collector is reduced by the cosine of the angle between the normal to the collector's surface and the Sun. This angle, called incidence angle (θi), can be illustrated by Figure 1.

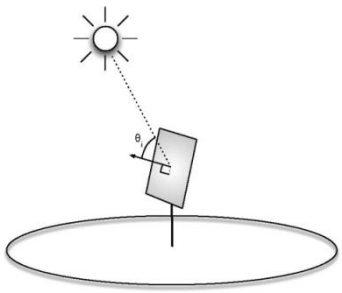

Fig.1. Incidence angle illustration.

Solar irradiance on the Earth's surface can be decomposed in two components: direct solar irradiance (G_b) - solar irradiance that comes directly from the Sun's disk; diffuse solar irradiance (G_d) - solar irradiance that comes from all directions over the entire sky.

The direct solar irradiance in an arbitrarily oriented surface can be written as:

$$G_b = G_{bMAX}\cos\theta_i \quad (6)$$

where Gb_{MAX} corresponds to the maximum component of direct solar irradiance.

On the other hand, the cosine of the incidence angle in an arbitrarily oriented surface can be described through the dot product of two vectors: the Surface-Sun vector (S) - unit vector pointing from a given location on Earth's surface to the Sun and the Collector-Sun vector (N) - unit vector normal to the collecting surface. Since these are unit vectors it is possible to write:

$$\cos\theta_i = \mathbf{S}\bullet\mathbf{N} \quad (7)$$

Surface-Sun vector

As we have seen, the angle A corresponds to the azimuth angle and a to the solar altitude. These angles can be defined through three other variables: the hour angle (ω), the declination angle (δ) and the latitude angle (ϕ). The first two reflect the time dependence of the vector S, while f is responsible for its geographic variation. To do that it is necessary to apply a mathematical translation to the surface-Sun vector in order to change its coordinate system to the centre of the Earth, being possible to write the following equations (where all angles are in degrees) [9]:

$$\alpha = \sin^{-1}\left(\sin\delta\sin\phi + \cos\delta\cos\omega\cos\phi\right) \quad (8)$$

$$\begin{aligned} A &= 180^{o} - A' \quad \text{if} \quad \cos\omega \geq \frac{\tan\delta}{\tan\phi} \\ A &= 360^{o} + A' \quad \text{if} \quad \cos\omega < \frac{\tan\delta}{\tan\phi} \end{aligned} \quad (9)$$

$$A' = \sin^{-1}\left(\frac{-\cos\delta\sin\omega}{\cos\alpha}\right) \quad (10)$$

Collector-Sun vector

The Collector-Sun vector can be defined taking into account the topology and dynamics of the photovoltaic collection system. In the fixed system case, the collection device is static and it is assumed that it is tilted at an angle b with the horizontal and oriented according to an azimuth angle z; in the two axes tracking system case, one admits that the system is capable of orienting the collecting surface so that its normal is perfectly aligned with the position of the Sun in the sky.

Incidence angle computation

Recalling equation (7) it is possible to calculate the incidence angle through manipulation of surface-Sun and collector-Sun vectors.

1) Fixed systems: The solar incidence angle in a fixed collection surface is computed as follows:

$$\cos\theta_i = \sin\alpha\cos\beta + \cos\alpha\sin\beta\cos(\zeta - A) \quad (11)$$

Using equations (8) and (9), it is also possible to write the incidence angle as a function of hour, declination and latitude angles, making possible, together with equations (4) and (5), its determination based on the date, time and location as can be seen in equation (12):

$$\begin{aligned}\cos\theta_i = {} & \cos\beta(\sin\delta\sin\phi + \cos\delta\cos\phi\cos\omega) - \\ & -\cos\delta\sin\omega\sin\beta\sin\zeta + \\ & +\sin\beta\cos\zeta(\sin\delta\cos\phi - \cos\delta\sin\phi\cos\omega)\end{aligned} \quad (12)$$

2) Two axes tracking systems: Since two axes full tracking systems are designed to keep S and N collinear, the incidence angle is always zero and:

$$\cos\theta_i = 1 \quad (13)$$

More details about solar geometry and incidence angle computation can be found in [9] and [11].

2.3. Maximum direct and diffuse irradiance prediction model

Given the topics covered in the last two sub-sections and knowing the direct irradiance received in a given area, it is possible to calculate, for each instant, its maximum component through:

$$G_{bMAX} = \frac{G_b}{\cos\theta_i} \quad (14)$$

The two axes solar tracking photovoltaic systems are designed to guide the collection surface so that its normal is perfectly aligned with the Sun's position in the sky, always processing the maximum component of direct incident irradiance.

We remark that the maximum global irradiance to be used as input to the PV output power forecast model should be G*t:

$$G_t^* = G_{bMAx} + G_d = \frac{G_b}{\cos\theta_i} + G_d \quad (15)$$

If the available data concern only the total irradiance, $G_t = G_b + G_d$, the direct and diffuse irradiance should be split apart. For that purpose, a diffuse irradiance analytical model can be used [12] as shown in equation (16):

$$G_d = \cos\theta_z\left(k_1 G_0 + k_2 G_{bMAX}\right) \quad (16)$$

In equation (16), $G_0 = Gsc\ (1 + 0{,}034 \cos x)$, k_1, k_2 are given constants and G_{sc} is the solar constant.

After some algebraic manipulation it is possible to obtain the following expression to compute the diffuse irradiance as a function of the total irradiance G_t:

$$G_d = \frac{\cos\theta_z\left(k_1 G_0 + \dfrac{k_2 G_t}{\cos\theta_i}\right)}{1 + k_2\dfrac{\cos\theta_z}{\cos\theta_i}} \quad (17)$$

The direct irradiance may be then straightforward calculated as: $G_b = G_t - G_d$.

Using the calculation model established to determine the incidence angle on a fixed surface, it is possible, using the proposed methodology, to calculate the maximum global incident irradiance on that surface. This data, together with data concerning the module temperature, can feed a model for predicting the power output of a photovoltaic system, so that one can estimate the energy produced by a PV system equipped with two axes solar tracking.

We should mention that the module temperature can be straightforward obtained from the ambient temperature using the NOCT (Normal Operating Cell Temperature) parameter available in the manufacturer datasheet.

3. PV Power Output Prediction Model

3.1. Electrical model

A typical silicon solar cell consists of a p-n junction, which has a diode characteristic (representing the p-n junction). This characteristic can be derived from standard solid state physics:

$$I = I_0\left(e^{\frac{V_A}{mV_T}} - 1\right) \quad (18)$$

As far as equation (18) is concerned, I is the current through the diode at the applied voltage VA, VT is a constant called thermal voltage, I0 is the diode reverse saturation current and m is the diode ideality factor, which depends on the type, doping density and quality of the semiconductor material.

If the junction is illuminated, an additional current, the light generated current IL is added, resulting in:

$$I = I_L - I_0\left(e^{\frac{V_A}{mV_T}} - 1\right) \quad (19)$$

Based on equation (19) it is possible to create an equivalent circuit of this type of solar cell (Figure 2) containing the following components: a current source (I_L), representing the light generated current, a diode (D), representing the p-n junction and the resistors R_s and R_{sh}, representing the resistive nature components of the cell.

The series resistance, R_s, describes the voltage drop, observed experimentally, due to external contacts. Similarly, the observed leakage currents can be described by the parallel resistance R_{sh}.

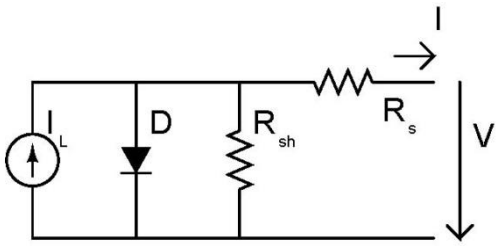

Fig. 2. Equivalent circuit of a photovoltaic cell (one diode and five parameters model).

Based on the circuit of Figure 2, the mathematical model of a photovoltaic cell can be defined in accordance with the following expression:

$$I = I_L - I_0\left(e^{\frac{V+R_sI}{mV_T}} - 1\right) - \frac{V+R_sI}{R_{sh}} \quad (20)$$

3.2. Model parameters determination

To use the model of Figure 2 it is necessary to determine the parameters (I_L, I_0, m, R_s e R_{sh}) that produce the best fit to a given photovoltaic cell operating under certain conditions.

There are several ways to determine these parameters. One approach is to test the photovoltaic cell under certain conditions of temperature and irradiance for various values of applied voltage. This experience results in a current-voltage characteristic that can be adjusted to the equation of the proposed model by means of a curve fitting tool. However, this approach involves laboratory testing of the cell, which in many cases is neither practical nor feasible. An alternative to this method is the determination of model parameters based on information provided by cells' manufacturers. This type of approach is presented in this sub-section.

There is a set of measurements, normally provided by manufacturers of PV devices that characterize the photovoltaic cells. Usually, this information comprises: short circuit current (I_{SC}), open circuit voltage (V_{OC}), voltage at maximum power point (V_{MAX}), current at maximum power point (I_{MAX}), temperature coefficient of short circuit current (μ_{ISC}) and temperature coefficient of open circuit voltage (μ_{VOC}). These values refer to tests carried out under special conditions, called standard test conditions (STC), where: Tr = 25º C, Gr = 1000 Wm^{-2} and AM^r = 1,5. The superscript "r" is used to identify these conditions.

Determination of model parameters is accomplished by analysing equation (20) for a particular set of conditions, as follows:

Starting equations

Equation (20) can be written for three key points of the I-V characteristic, the short circuit point, the open circuit point and the maximum power point, as follows:

$$I_{SC} = I_L - I_0 e^{\frac{R_sI_{SC}}{mV_T}} - \frac{R_sI_{SC}}{R_{sh}} \quad (21)$$

$$0 = I_L - I_0 e^{\frac{V_{OC}}{mV_T}} - \frac{V_{OC}}{R_{sh}} \quad (22)$$

$$I_{MAX} = I_L - I_0 e^{\frac{V_{MAX}+R_sI_{MAX}}{mV_T}} - \frac{V_{MAX}+R_sI_{MAX}}{R_{sh}} \quad (23)$$

In silicon devices, the dark saturation current is very small compared to the exponential term, so in the above equations we have considered that

$$I_0 \exp\left[\left(V+R_sI\right)/\left(mV_T\right)\right] >> I_0$$

Knowing that at the point of maximum power, the derivative of the equation that defines the power (P) is zero (maximum of primitive function), it is possible to write:

$$\left.\frac{dP}{dV}\right|_{\substack{V=V_{MAX}\\I=I_{MAX}}} = \left.\left(I + \frac{dI}{dV}V\right)\right|_{\substack{V=V_{MAX}\\I=I_{MAX}}} = 0 \quad (24)$$

It is also known empirically that the resistance R_{sh} is related to the I-V characteristic as:

$$\left.\frac{dI}{dV}\right|_{I=I_{SC}} = -\frac{1}{R_{sh}} \quad (25)$$

Equations manipulation

Substituting equation (22) in equation (21) yields:

$$I_{SC} = I_0\left(e^{\frac{V_{OC}}{mV_T}} - e^{\frac{R_sI_{SC}}{mV_T}}\right) + \frac{V_{OC}-R_sI_{SC}}{R_{sh}} \quad (26)$$

Since , it is possible to re-write equation (26) as:

$$I_0 = \left(I_{SC} - \frac{V_{OC}-R_sI_{SC}}{R_{sh}}\right)e^{\frac{-V_{OC}}{mV_T}} \quad (27)$$

Replacing (22) and (27) in equation (20) (again neglecting the term "-1") one can obtain:

$$I = I_{SC} - \frac{V+R_sI-R_sI_{SC}}{R_{sh}} - \left(I_{SC} - \frac{V_{OC}-R_sI_{SC}}{R_{sh}}\right)e^{\frac{V+R_sI-V_{OC}}{mV_T}} \quad (28)$$

To develop equation (24) it is necessary to differentiate equation (28) in order to the voltage V. However, this is a

transcendental equation and a non-analytical approach is needed. Since $I = f(I,V)$ the differential operator can be used to obtain:

$$dI = dI\frac{\partial f(I,V)}{\partial I} + dV\frac{\partial f(I,V)}{\partial V} \quad (29)$$

and the derivative of the current with respect to voltage results in:

$$\frac{dI}{dV} = \frac{\dfrac{\partial f(I,V)}{\partial V}}{1-\dfrac{\partial f(I,V)}{\partial I}} \quad (30)$$

Substituting (30) in (24) yields, where f(I,V) can be replaced by equation (28):

$$\left.\frac{dP}{dV}\right|_{\substack{V=V_{MAX}\\I=I_{MAX}}} = 0 = I_{MAX} + \left.\frac{\dfrac{\partial f(I,V)}{\partial V}}{1-\dfrac{\partial f(I,V)}{\partial I}}\right|_{\substack{V=V_{MAX}\\I=I_{MAX}}} V_{MAX} \quad (31)$$

Developing, it is possible to obtain:

$$\left.\frac{dP}{dV}\right|_{\substack{V=V_{MAX}\\I=I_{MAX}}} = 0 = I_{MAX} + \frac{-\dfrac{\left(R_{sh}I_{SC}-V_{OC}+R_sI_{SC}\right)e^{\frac{V_{MAX}+R_sI_{MAX}-V_{OC}}{mV_T}}}{mV_T\,R_{sh}} - \dfrac{1}{R_{sh}}}{1+\dfrac{R_s\left(R_{sh}I_{SC}-V_{OC}+R_sI_{SC}\right)e^{\frac{V_{MAX}+R_sI_{MAX}-V_{OC}}{mV_T}}}{mV_T\,R_{sh}} + \dfrac{R_s}{R_{sh}}}V_{MAX} \quad (32)$$

On the other hand, combining equation (25) with equation (30) yields:

$$\left.\frac{dI}{dV}\right|_{I=I_{SC}} = \left.\frac{\dfrac{\partial f(I,V)}{\partial V}}{1-\dfrac{\partial f(I,V)}{\partial I}}\right|_{I=I_{SC}} = -\frac{1}{R_{sh}} \quad (33)$$

Developing comes that:

$$\left.\frac{dI}{dV}\right|_{I=I_{SC}} = -\frac{1}{R_{sh}} = \frac{-\dfrac{\left(R_{sh}I_{SC}-V_{OC}+R_sI_{SC}\right)e^{\frac{R_sI_{SC}-V_{OC}}{mV_T}}}{mV_T\,R_{sh}} - \dfrac{1}{R_{sh}}}{1+\dfrac{R_s\left(R_{sh}I_{SC}-V_{OC}+R_sI_{SC}\right)e^{\frac{R_sI_{SC}-V_{OC}}{mV_T}}}{mV_T\,R_{sh}} + \dfrac{R_s}{R_{sh}}} \quad (34)$$

Finally, substituting (22) and (27) in equation (23), one can write:

$$I_{MAX} = I_{SC} - \frac{V_{MAX}+R_sI_{MAX}-R_sI_{SC}}{R_{sh}} - \left(I_{SC}-\frac{V_{OC}-R_sI_{SC}}{R_{sh}}\right)e^{\frac{V_{MAX}+R_sI_{MAX}-V_{OC}}{mV_T}} \quad (35)$$

Using equations (32), (34) and (35), the set of measurements provided by cells' manufacturers and a numerical method for solving systems of nonlinear equations it is possible to obtain the parameters m, Rs e Rsh for the standard test conditions. Once determined these parameters, one can solve the system of equations formed by (21) and (22) and obtain the remaining parameters, I_L e I0 (also for STC).

3.3. Temperature and irradiance influence

Once the model parameters for standard test conditions are determined, it is possible to modify them to account for irradiance and cell temperature. Therefore, an I-V characteristic that reflects the cell's electrical behaviour under specific conditions of temperature and irradiance is obtained for each cell operating point.

It is assumed that the parameters m, R_s and R_{sh} do not depend on cell temperature or irradiance. On the other hand, I_0 and I_L can be written as function of the variables I_{SC} and V_{OC}, and as function of the model parameters m, R_s and Rsh as shown in equations (27) and (22). Taking advantage of this fact, it is possible to study the influence of temperature and irradiance on I_0 and I_L by analysing the behaviour of ISC and V_{OC} when subjected to temperature and irradiance variations, according to the following equations:

$$I_{SC}(G,T) = \frac{G}{G^r}\left[I_{cc}^r + \mu_{I_{SC}}\left(T-T^r\right)\right] \quad (36)$$

$$V_{OC}(G,T) = V_{OC}^r + \mu_{V_{OC}}\left(T-T^r\right) + mV_T\ln\left(\frac{G}{G^r}\right) \quad (37)$$

Once the short circuit current and open circuit voltage for a generic set of conditions of irradiance and temperature (using (36) and (37), respectively) have been determined, it is possible to feed equations (23) and (27) in order to obtain the respective parameters I_L and I_0.

3.4. Electrical power

Now it is possible to estimate the electrical output power of a cell. For this, expression (24) should be written as:

$$\left.\frac{dI}{dV}\right|_{\substack{V=V_{MAX}\\I=I_{MAX}}} = -\frac{I_{MAX}}{V_{MAX}} \quad (38)$$

Using the same approach as in equations (29) and (30), it is possible to develop equation (38) and obtain equation (39).

The PV system is equipped with a Maximum Power Point Tracker (MPPT) that ensures it is working at maximum power point. As so, it is possible to solve the system of nonlinear equations composed by (35) and (39) to obtain V_{MAX} and I_{MAX} and consequently the cell's output power.

$$\frac{-\frac{\left(R_{sh}I_{SC}-V_{OC}+R_sI_{SC}\right)e^{\frac{V_{MAX}+R_sI_{MAX}-V_{OC}}{mV_T}}}{mV_T R_{sh}}-\frac{1}{R_{sh}}}{1+\frac{R_s\left(R_{sh}I_{SC}-V_{OC}+R_sI_{SC}\right)e^{\frac{V_{MAX}+R_sI_{MAX}-V_{OC}}{mV_T}}}{mV_T R_{sh}}+\frac{R_s}{R_{sh}}}=-\frac{I_{MAX}}{V_{MAX}} \quad (39)$$

3.5. PV module electrical model

The electrical model developed in this section relates to the behaviour of a single photovoltaic cell. However, it is possible to extend this model to characterize the electrical quantities of a photovoltaic module. For this, one should consider that a photovoltaic module corresponds to an equivalent cell, in which all parameters refer to a module and not to an individual cell.

Once the electrical model that allows relating the input variables, temperature and solar irradiance, with the current and voltage in the terminals of a photovoltaic module is defined, it is possible to establish a method to define its I-V characteristic. An algorithm to predict the power delivered by that device can also be developed.

In both tasks, the initial approach is common. In the first place it is necessary to calculate the parameters of the presented model in the standard test conditions. Then, for each pair of values of temperature and solar irradiance, the referred parameters must be modified. Note that the ambient temperature must be converted into photovoltaic module temperature using a temperature model.

4. Model Validation

In this section, experimental data is used to validate both the maximum global irradiance and PV power output prediction models presented in this paper so far. For this, data referring to a day of operation of a photovoltaic testing system has been analysed, as well as readily available data from a solar atlas (PVGIS) is used to strengthen the obtained results.

4.1. Single day validation

In order to validate the approach developed in this paper, data referring to a day of operation of a photovoltaic testing system has been analysed. The PV testing system consists of two sub-systems, installed side by side, each one composed by eight BP5170S (P_p = 170 Wp) photovoltaic modules connected to a Fronius IG15 1300 W inverter. One of the sub-systems is fixed, south oriented, with a slope of 30º, and the other one has a two axes tracking system that allows it to be always oriented towards the Sun.

With the PV testing system's software it is possible to create a database with 5 minutes average values of total incident irradiance, ambient temperature and delivered power to the grid for each sub-system.

Using the fixed sub-system total irradiance measured data and the global irradiance prediction model proposed in this paper, one can estimate the maximum global irradiance as received by an equivalent two axes tracking system; then, these results can be compared with the actual recorded irradiance received by the sub-system with tracking. In a second phase, it is possible to input the forecasted global irradiance to the one diode and five parameters PV power output model and evaluate the global irradiance prediction model in terms of produced energy delivered to the grid. A scheme of this validation process is shown in Figure 3.

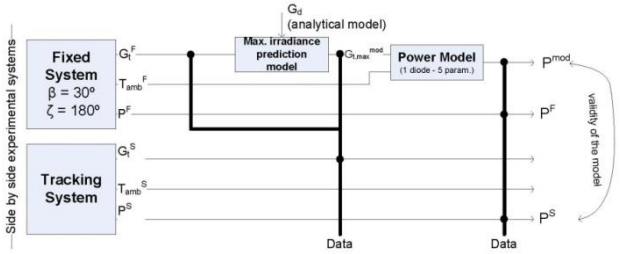

Fig. 3. Schematic of the validation process used - single day validation.

In Figure 4 is shown the one day measured irradiance received by the fixed testing sub-system, as well as the computed irradiance received by an equivalent two axes tracking system. It is also depicted the irradiance recorded by the experimental two axes tracking sub-system.

Figure 5 shows the representation of the error between the two axes tracking system irradiance prediction model and experimental results. It is also indicated in Figure 4 the resulting average error.

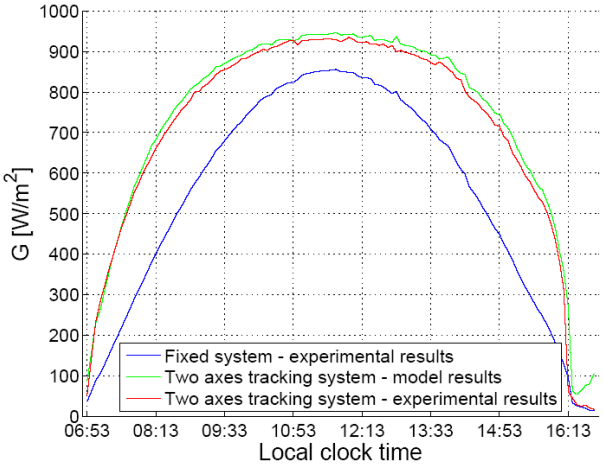

Fig. 4. Irradiance charts for the fixed system (experimental results) and for the two axes tracking system (model and experimental results).

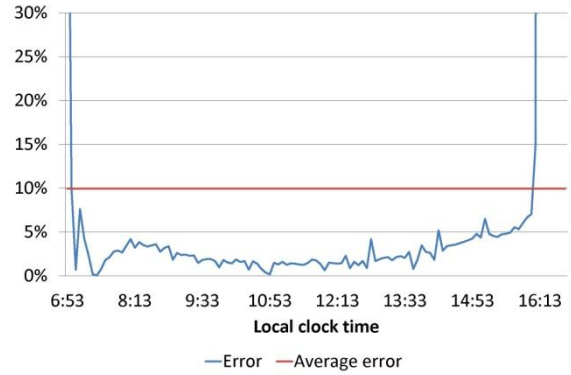

Fig. 5. Error between the two axes tracking system irradiance prediction model and the two axes tracking system experimental irradiance results.

Figure 6 concern the application of the five parameter PV power model to the irradiance data generated by the two axes tracking system irradiance prediction model, referring to one day of operation.

In Table I the energy as measured by the experimental systems (fixed and with tracking) and the computed energy delivered to the grid that results from the application of the prediction models are presented. It should be noted that to compute the energy delivered to the grid, appropriate models for the MPPT and the inverter have been included [13].

In broad terms, we can state that the comparisons resulting from the validation process indicate that, for this day, the proposed models give satisfactory results.

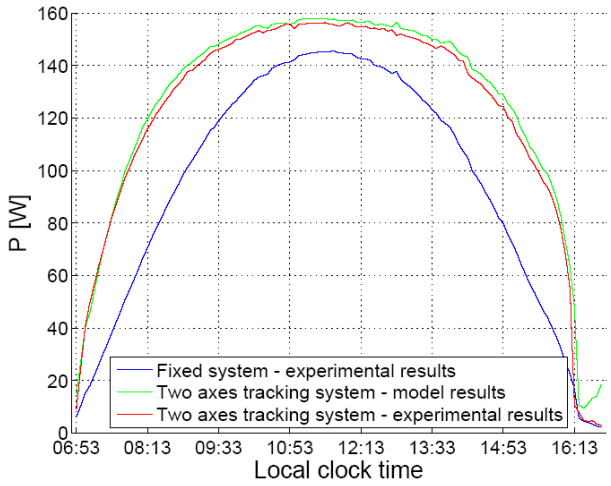

Fig. 6. Power charts for the fixed system (experimental results) and for the two axes tracking system (model and experimental results).

Table 1. Energy results (in kWh) of maximum incident irradiance prediction model validation.

Fixed system - experimental results	0,94
Two axes tracking system - model results	1,24
Two axes tracking system - experimental results	1,2
Improvement (fixed *vs* two axes tracking)	27,66%
Error (two axes tracking - model *vs* experimental results)	3,33%

Regarding the irradiance prediction of the tracking system, the results show an average error of 10% throughout the day in question. Figures 4 and 5 illustrate that, during most part of the day, the model provides results with an error of less than 5%. However, for smaller values of irradiance (initial and final parts of the day) the model gives incorrect results, making a decisive contribution to the worsening of the average error. This behaviour is due to the numerical error associated with the term $G_b/\cos\theta_i$, which tends to assume high values for qi near 90º.

Furthermore, in the power and energy analysis, Figure 6 and the results of Table I show substantially smaller errors, around 3%. This is because the error of the irradiance model is large for low values of irradiance, but small in periods of high irradiance; therefore, their contribution to the error of the power model is not too significant. Hence, the power error is perfectly acceptable given the modest complexity of the presented model.

Table I also indicates that the tracking system produces about 28% more energy than the fixed system. Although it is not possible to generalize regarding the performance of tracking systems, because only a single day of operation has been analysed, the improvement observed motivates a more enlightening study on the subject, which is one of the objectives of the following section.

4.2. Full year validation

In this section, readily available data from a solar atlas is used to strengthen the validation previously carried out. The collected data is also used to evaluate two axes tracking system performance against a fixed system, over the course of a full year of operation. The solar atlas used is the PVGIS atlas, a solar irradiance database developed under the auspices of European Union available at http://re.jrc.ec.europa.eu/pvgis.

Among its many features, this atlas allows to choose a location (in Europe or in some places of Africa and south-west Asia), set the inclination and orientation of a fixed plan and, for a typical day of each month of the year, obtain the following data: global and diffuse irradiance on the defined fixed plane; global and diffuse irradiance on two axes tracking plane; average daytime ambient temperature.

In this sub-section, the referred atlas is used to obtain irradiance data (global and diffuse) on a flat surface facing south with a slope of 30º in the Lisbon area. It is also collected homologous data for two axes tracking plane and average daytime ambient temperature. Using these data and an approach identical to the one used in the single day validation, it is possible to feed the model of maximum global irradiance estimation received by an equivalent two axes tracking system and compare the obtained results with the tracking results provided by the atlas (in a process that can be summarized by the content of Figure 7). This procedure is repeated for a typical day of each month of the year.

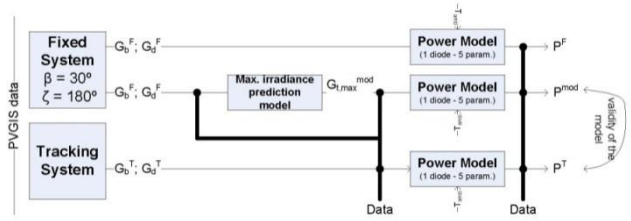

Fig. 7. Schematic of the validation process used - full year validation

To evaluate the power performance of the two axes tracking systems compared to fixed systems, this study considers the existence of a BP5170S photovoltaic module, identical to the one mentioned before. Once again, using the one diode and five parameters model, it is possible to obtain a power diagram for each one of the irradiance profiles considered in the previous sub-section.

In Table II it is presented the results of the computed energy based on data respecting a fixed system and data from the system with tracking, both for a typical day of operation of each month, using the atlas irradiance data and the proposed irradiance estimation model. It is also computed the energy per month, considering that all days are typical.

Table 2. Fixed system and two axes tracking system annual energy comparison (AID - Atlas Irradiance Data, MID - Model Irradiance Data)

	A	B	C	D	E	F	G
Jan	3,8	0,59	0,78	0,76	18,36	24,24	23,48
Feb	2,88	0,65	0,83	0,81	18,25	23,11	22,57
Mar	4,44	0,93	1,2	1,16	28,95	37,12	35,83
Apr	6,7	0,95	1,22	1,18	28,35	36,54	35,29
May	8,86	1,04	1,39	1,33	32,3	43,15	41,16
Jun	13,17	1,1	1,56	1,44	33,13	46,69	43,24
Jul	12,56	1,13	1,59	1,48	35,06	49,26	45,93
Aug	7,99	1,11	1,5	1,43	34,5	46,45	44,37
Sep	5,77	1,02	1,32	1,27	30,46	39,68	37,97
Oct	5,33	0,84	1,08	1,04	26,08	33,53	32,12
Nov	4,59	0,59	0,77	0,74	17,77	23,12	22,25
Dec	4,33	0,54	0,72	0,69	16,65	22,23	21,41
Total	-	-	-	-	319,85	425,1	405,59
Average	6,7	-	-	-	-	-	-

A - Irradiance average error [%]
B - Energy of the fixed system (AID) per typical day [kWh]
C - Energy of the tracking system (AID) per typical day [kWh]
D - Energy of the tracking system (MID) per typical day [kWh]
E - Energy of the fixed system (AID) per month [kWh]
F - Energy of the tracking system (AID) per month [kWh]
G - Energy of the tracking system (MID) per month [kWh]

All this information is summarized in Figure 8, which presents a comparison of the annual energy produced by the fixed system (using atlas irradiance data) and the two axes tracking system (using both model and atlas irradiance data).

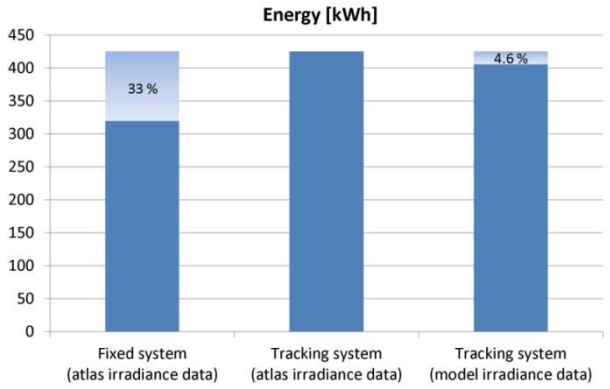

Fig. 8. Comparison of annual energy produced by the fixed system (using atlas irradiance data) and the two axes tracking system (using both forecast models and atlas irradiance data).

Regarding the values presented in column "A" of Table II, one can conclude that the irradiance average error found in the single day validation simulation (10%) is in pace with the results obtained for the monthly typical day validation. Furthermore, this exercise allows validating the global irradiance prediction model developed in this paper, from the standpoint of annually produced energy. As it is evident in the chart of Figure 8, model results allow obtaining an annual produced energy value with an error of 4,6% when compared to the annual value generated with PVGIS atlas irradiance data for a two axes tracking plane. It is important to note that the error of the one diode and five parameters model, used to obtain power from irradiance and temperature, affect both results similarly.

Considering the set of obtained results, it is also possible to conclude that systems with two axes tracking show a gain of about 33% compared to the corresponding fixed system installed south oriented and with a slope of 30º, in the Lisbon area. Note that these results cannot be blindly extended to other geographies, since the solar geometry and solar irradiance data are different. However, one can generalize the calculation process, being possible to infer about the gain for different locations and orientations. It is also called the attention to the fact that the power consumption by the tracking device can be about 3% of the increased energy. This factor should be subtracted from the obtained gain to determine the real gain of the system. To improve this analysis, one can also perform a study regarding the type of control used and the relationship between control project options and energy gain obtained, in accordance with what is presented in [14].

5. Conclusion and Outlook

In this paper, a model to compute the maximum global irradiance as collected by a two axes solar tracking PV system has been proposed. The prediction model is based on readily available data concerning total incident irradiance in an arbitrary oriented surface. To that end, the main concepts related to solar geometry and incidence angle computation have been recalled. The developed prediction model has been validated with the help of experimental data collected in a test facility, presenting an error around 5%, during most of

the selected comparison day. This is a good indication of the adequacy of the proposed model. Also, a PV power output prediction model has been presented in this paper. This a one diode and five parameters model, based solely on datasheet information. The model takes account for variations in both irradiance and temperature.

The aggregate of both models have been used to compute the energy delivered to the grid, in a selected day, by a two axes tracking PV system. The comparison with experimental energy data showed that the error is around 3%, which, once again, is a good result, as far as the models validation is concerned.

Extended validation using yearly data from a solar atlas has been carried out, which broadly confirmed the results of the one day experimental validation. Moreover, the study presented in this paper has enabled the confirmation of other results presented in the literature [14] stating that the improvement of a two axes tracking system power performance against a fixed system is about 30%.

Acknowledgements

The authors deeply acknowledge EDP Inovação for making available the experimental data of the PV test system.

References

[1] B. Fry, "Simulation of Grid-Tied Building Integrated Photovoltaic Systems," Master's thesis, University of Wisconsin-Madison, 1998.

[2] J. Crispim, M. Carreira, R. Castro, "Validation of photovoltaic electrical models against manufacturers data and experimental results," in IEEE International Conference on Power Engineering, Energy and Electrical Drives (POWERENG'07), Setubal, 2007.

[3] A. N. Celik, N. Acikgoz, "Modelling and experimental verification of the operating current of mono-crystalline photovoltaic modules using four- and five-parameter models," Applied Energy, vol.84, no.1, 2007.

[4] W. Shen, Y. Ding, F. H. Choo, P. Wang, P. C. Loh, K. K. Tan, "Mathematical model of a solar module for energy yield simulation in photovoltaic systems," in International Conference on Power Electronics and Drive Systems, 2009 (PEDS 2009), 2009.

[5] V. L. Brano, A. Orioli, G. Ciulla, A. D. Gangi, "An improved five parameter model for photovoltaic modules," Solar Energy Materials and Solar Cells, vol.94, no.8, 2010.

[6] J. Gow, C. Manning, "Development of a photovoltaic array model for use in power-electronics simulation studies," IEE Proceedings - Electric Power Applications, vol.146, no.2, 1999.

[7] D. Sera, R. Teodorescu, P. Rodriguez, "PV panel model based on data-sheet values," in IEEE International Symposium on Industrial Electronics, 2007.

[8] W. D. Soto, S. Klein, W. Beckman, "Improvement and validation of a model for photovoltaic array performance," Solar Energy, no.80, 2006.

[9] W. B. Stine, M. Geyer, Power from the Sun, 2001, Accessed on August 2, 2011, Available at <http://www.powerfromthesun.net/index.html>

[10] H. M. Woolf, "On the computation of solar evaluation angles and the determination of sunrise and sunset times", National Aeronautics and Space Administration, Report NASA TM-X-164, 1968.

[11] A. Coelho, "New trends in photovoltaic systems - Modelling power output with solar tracking," Master's thesis, IST - Technical University of Lisbon, 2010.

[12] B. Liu, R. Jordan, "The interrelationship and characteristic distribution of direct, diffuse and total solar radiation," Solar Energy, vol.4, no.1, 1960.

[13] B. Bletterie, R. Bruendlinger, S. Spielauer, "Quantifying dynamic MPPT performance under realistic conditions," in 21st European Photovoltaic Solar Energy Conference, 2006.

[14] C. Alexandru, "The design and optimization of photovoltaic tracking mechanism," in International Conference on Power Engineering, Energy and Electrical Drives (POWERENG'09), Caparica, 2009.